

The Interpretation and Implication of the Afterglow of GRB 060218

Yizhong Fan^{1,2,3*}, Tsvi Piran¹ † and Dong Xu⁴

¹*The Racah Inst. of Physics, Hebrew University, Jerusalem 91904, Israel*

²*Purple Mountain Observatory, Chinese Academy of Science, Nanjing 210008, China*

³*National Astronomical Observatories, Chinese Academy of Sciences, Beijing 100012, China*

⁴*Dark Cosmology Centre, Niels Bohr Institute, University of Copenhagen, Juliane Maries Vej 30, 2100 Copenhagen, Denmark*

Accepted Received; in original form

ABSTRACT

The nearby GRB 060218/SN 2006aj was an extremely long, weak and very soft GRB. It was peculiar in many aspects. We show here that the X-ray, ultraviolet/optical and radio afterglow of GRB 060218 have to be attributed to different physical processes arising from different emission regions. From the several components in this burst's afterglow only the radio afterglow can be interpreted in terms of the common external shock model. We infer from the radio that the blast wave's kinetic energy was $\sim 10^{50}$ erg and the circumburst matter had a constant rather than a wind profile. The lack of a “jet break” up to 22 days implies that the outflow was wide $\theta_j > 1$. Even though the late X-ray afterglow decays normally it cannot result from an external shock because of its very steep spectrum. Furthermore, the implied kinetic energy would have produced far too much radio. We suggest that this X-ray afterglow could be attributed to a continued activity of the central engine that within the collapsar scenario could arise from fall-back accretion. “Central engine afterglow” may be common in under-luminous GRBs where the kinetic energy of the blast wave is small and the external shock does not dominate over this component. Such under-luminous GRBs might be very common but they are rarely recorded because they can be detected only from short distances.

Key words: Gamma Rays: bursts—ISM: jets and outflows—radiation mechanisms: nonthermal—X-rays: general

1 INTRODUCTION

GRB 060218 (Cusumano et al. 2006a) was a nearby ($z=0.033$, Mirabal & Halpern 2006; Cusumano et al. 2006b) burst associated with a bright type Ic broad-lines SN (Modjaz et al. 2006; Sollerman et al. 2006; Pian et al. 2006; Mirabal et al. 2006; Mizalli et al. 2006). It is distinguished in several aspects from other bursts: (i) It is very long ($T_{90} \sim 2000$ sec). (ii) The prompt γ -ray and X-ray luminosity is extremely low $\sim 10^{47}$ erg s⁻¹ (Sakamoto et al. 2006) and the overall isotropic equivalent γ -ray energy, $E_\gamma \sim 6 \times 10^{49}$ erg, is small compared to typical bursts. (iii) The prompt emission is very soft and it contains a soft thermal component in the X-ray band. The thermal emission begins at ~ 152 sec and continues up to $\sim 10^4$ sec. (iv) A second thermal component in the UV/optical band peaks at $t \sim 1$ day af-

ter the GRB trigger (Campana et al. 2006). (v) For $t > 0.1$ day, the XRT lightcurve is simple and is well described a single power-law decay $t^{-1.15}$ with no break (Campana et al. 2006). (vi) For $t > 1.8$ day, the 8.46 GHz radio afterglow lightcurve decays as $t^{-0.85}$ without break (Soderberg et al. 2006a). While the prompt emission is very different from a typical GRB and the optical emission is complicated by the appearance of the thermal bump and the supernova signal this last component, the X-ray and the radio afterglow, seem to be rather typical.

We focus here on the X-ray and the radio afterglow, and use them as keys to understand what has happened in this burst. The X-ray afterglow decays normally and this has led us to suggest, in an earlier draft of this paper, that it arose from a standard external shock. However, later it was revealed that the X-ray emission has a very steep spectra¹ that rules out an external shock origin. Furthermore, the

* Lady Davis Fellow, E-mail: yzf@pmo.ac.cn

† tsvi@phys.huji.ac.il

¹ The first XRT spectral index β_X was quite uncertain. For ex-

radio observations (Soderberg et al., 2006), that were also unknown at this stage, are incompatible with the kinetic energy required to produce the X-ray emission by an external shock. Instead we suggest that the X-ray afterglow could be attributed to a “central engine afterglow” resulting from a continued activity of the central engine, as suggested already in 1997 by Katz & Piran. We argue that such afterglow could be common in the under-luminous nearby GRBs (see section 2 for details).

The radio afterglow, on the other hand, can be interpreted in terms of the standard afterglow model. One can infer from it the kinetic energy, $E_k \sim 10^{50}$ erg, as well as the wide opening angle, $\theta_j > 1$, of the relativistic component of the ejecta. The association with a type Ic SN suggests that the progenitor was a WR-star (Campana et al. 2006). One expects, therefore, that the central engine is surrounded by a dense stellar wind, like the one seen in GRB 980425 that was associated with SN 98bw (Li & Chevalier 1999; Waxman 2004). However, the density nearest to the progenitor depends on the mass loss rate during the latest phases of the WR-star, which is unknown at present (Woosley, Zhang & Heger 2003). With the radio data, we show that a dense wind profile is not favored (see section 3 for details).

We examine possible sources for the thermal emission in section 4. Our conclusions and the implications for the GRB/SN connection are discussed in section 5.

2 THE LONG TERM X-RAY EMISSION FROM THE CENTRAL ENGINE

The late (> 0.1 day) X-ray afterglow is similar to the one seen in typical GRBs in its overall intensity as well as in the almost standard power law decay index $\alpha_X \sim -1.1$. However, the time averaged XRT spectral index $\beta_X = -2.2 \pm 0.2$ is too steep to be reproduced in the standard fireball model. For $\beta_X = -2.2 \pm 0.2$, the power-law distribution index of the shocked electrons $p = 5.4$ or 4.4 , depending on the X-ray band being below or above the cooling frequency ν_c . In the constant density circumburst medium case, the expected temporal index $\alpha = (2 - 3p)/4 < -2.8$ for $\nu_X > \nu_c$ otherwise $\alpha = 3(1 - p)/4 < -2.6$ (Sari, Piran & Narayan 1998; Piran 1999). In the wind case, the expected temporal index $\alpha = (2 - 3p)/4 < -2.8$ for $\nu_X > \nu_c$ otherwise $\alpha = (1 - 3p)/4 < -3$ (Chevalier & Li 2000). All are far from consistent with the observation ~ -1.1 .

The steep X-ray spectrum enables us to rule out the possibility that the X-ray emission arises due to inverse Compton. Sari & Esin (2001) have shown that the inverse Compton spectra is much shallower than -2.2 unless it is in the Klein-Nishina regime. Clearly the observed X-ray cannot be in the Klein-Nishina regime. Therefore we can rule out the possibility that the X-ray afterglow arises due to either synchrotron-self inverse Compton (SSC) or the inverse Compton scattering of the SN optical photons with the external forward shock electrons.

Even if we ignore the very steep spectrum, the external fireball model is still inconsistent because the X-ray emission is strong but the radio emission is very weak. Parameters

$E_k \sim 10^{51}$ erg, $\epsilon_e \sim 0.1$, $\epsilon_B \sim 0.01$ and $n \sim 1 \text{ cm}^{-3}$ are needed to reproduce the late X-ray emission ($t > 0.1$ day). With these parameters the resulting radio emission would have been about 1-2 orders brighter than the observation (Soderberg et al. 2006a).

An attractive alternative possibility for the production of the X-ray afterglow is the a continued activity of the central engine. This idea was first proposed by Katz & Piran already in 1997 and had been discussed in the context of GRB 970228 by Katz, Piran & Sari (1998). However, the agreement of the predictions of the external shock afterglow model with most subsequent multi-wavelength afterglows observation and in particular the smooth light curves seen in most afterglow lead to the understanding that afterglows are produced by external shocks. The energetic soft X-ray flares observe recently in many afterglows of *Swift* GRBs (O’Brien et al. 2006) lead Fan & Wei (2005) and Zhang et al. (2006) to re-introduce this model and to interpret these flares as arising from a continued activity of the central engine. When proposing the so-called “late internal shock” model, Fan & Wei (2005) speculated that in some GRBs, the X-ray and IR/optical afterglow might be attributed to different physical processes and thus from different regions. However, these X-ray flaring afterglows are quite different from the current long term power-law decaying lightcurve. This X-ray afterglow of GRB 060218 provides us the first indication for the power-law decaying lightcurves attributed to the central engine.

In the following we call the usual afterglow from the fireball’s external shocks the “fireball afterglow” or “afterglow” and the afterglow attributed to the long lived activity of the GRB central engine as the “central engine afterglow”. The central engine afterglow, besides those flares detected in *Swift* GRB X-ray afterglows, are expected to be detected in sub-luminous GRBs whose regular afterglows is weak and hence they do not over shine this activity. As such sub-luminous GRBs can be detected only from relatively short distances we will detect only few such bursts even if the total number of such under-luminous bursts is larger than the total number of regular GRBs. Alternatively, the “central engine afterglow” component may emerge if (i) The forward shock parameters ϵ_e and/or ϵ_B taken in eq. (4) are much smaller than the value normalized there; (ii) Some of or all the free parameters ϵ , f_x and f_b^{-1} taken in eqs. (1-3) have been underestimated significantly. In this case, a burst with a “central engine afterglow” component may be detectable at high redshift².

To estimate the possible flux from a “central engine afterglow” we consider, as an illustration, the “Type II collapsar” model of MacFadyen et al. (2001) to examine the possibility of a long term “central engine afterglow” in this scenario. As a conservative estimate, we take the lowest ac-

² A possible candidate is GRB 060210, a burst at $z \sim 4$ (Stanek et al. 2006). For this burst, the R-band flux is just about 10 times that of the X-ray (at 3.5 keV) and is decaying with time as $t^{-1.3}$ for $t > 500$ s. On the other hand, the XRT spectral index is -1.17 ± 0.04 (X. Y. Dai, 2006, private communication). It is thus quite difficult to interpret these data self-consistently within the standard external shock model. This inconsistency could be resolved if the X-ray emission is a “central engine afterglow” while the optical emission is the normal external shock afterglow.

ample, De Luca (2006) suggested that $\beta_X \sim -2.3 \pm 0.6$, whereas Cusumano et al. (2006b) give later $\beta_X \sim -2.3 \pm 0.2$.

cretion rate dM/dt presented in MacFadyen et al. (2001) (see their Fig. 5) i.e.,

$$dM/dt \sim 10^{-6} t_{d,-1}^{-5/3} M_{\odot} \text{ s}^{-1}, \quad (1)$$

where t_d represents the observer's time in units of day. Here and throughout this text, the convention $Q_x = Q/10^x$ has been adopted in cgs units. Following MacFadyen et al. (2001), we take an energy conversion coefficient $\epsilon \sim 0.001 - 0.01$ and the beam correction factor $f_b \sim 0.01 - 1$, (note that for this particular burst $f_b \sim 1$) thus the outflow luminosity can be estimated by

$$L \sim \epsilon (dM/dt) c^2 / f_b \sim 2 \times 10^{46} \text{ erg s}^{-1} \epsilon_{-3} f_{b,-1}^{-1} t_{d,-1}^{-5/3}. \quad (2)$$

Assuming that the fraction of the outflow converted into soft X-ray emission is $f_x \sim 0.01 - 0.1$ and for a luminosity distance $D_L \sim 10^{27}$ cm, the XRT flux

$$\begin{aligned} F_x &\sim f_x L / D_L^2 \\ &\sim 2 \times 10^{-10} \epsilon_{-3} f_{x,-2} f_{b,-1}^{-1} t_{d,-1}^{-5/3} \\ &\quad D_{L,27}^{-2} \text{ erg s}^{-1} \text{ cm}^{-2}. \end{aligned} \quad (3)$$

On the other hand, the forward shock X-ray emission is expected to be (Fan & Piran 2006a):

$$\begin{aligned} F_x &\sim 3 \times 10^{-12} \text{ ergs s}^{-1} \text{ cm}^{-2} (1+z)^{(p+2)/4} D_{L,27}^{-2} \\ &\quad \epsilon_{B,-2}^{(p-2)/4} \epsilon_{e,-1}^{p-1} E_{k,50}^{(p+2)/4} (1+Y)^{-1} t_{d,-1}^{(2-3p)/4}, \end{aligned} \quad (4)$$

where E_k is the isotropic equivalent energy of the outflow powering the afterglow, ϵ_e and ϵ_B are the fraction of shock energy given to the electrons as well as magnetic field. To get this and the following numerical coefficients, we take $p = 2.3$. $Y = (-1 + \sqrt{1 + 4\eta\eta_{KN}\epsilon_e/\epsilon_B})/2$ is the Compton parameter, where $\eta = \min\{1, (\nu_m/\nu_c)^{(p-2)/2}\}$ (Sari, Narayan & Piran 1996; Wei & Lu 1998), $0 \leq \eta_{KN} \leq 1$ is a coefficient accounting for the Klein-Nishina effect (Fan & Piran 2006a).

Comparing eq. (3) and (4) we see, as one could expect, that if the GRB outflow is significantly less energetic ($E_k \sim 10^{50}$ erg) than typical GRB ($E_k \sim 10^{53}$ erg), the ‘‘central engine afterglow’’ component dominates. So the central engine afterglow may be common for the sub-luminous GRBs. This prediction could be tested in the coming months or years.

Note that in this particular model the temporal decay $(-5/3)$ is too steep as compared with the observations of -1.1 . However this temporal decay (Eq. 3) is dictated simply by the accretion rate used in Eq. (1) and surely, there is enough freedom to expect a different slope there.

3 THE LATE RADIO AFTERGLOW: CONSTRAINT ON THE DENSITY PROFILE OF THE MEDIUM

Multi-wavelength radio data have been presented in Soderberg et al. (2006a). There are 11 detections, 8 of which are at 8.46 GHz, ranging from 1.8 – 22 days. The good quality 8.46 GHz lightcurve can be well fitted by a single power law $t^{-0.85}$. This decline slope (-0.85) is significantly different from that of GRB 980425 (~ -1.5). The radio emission is very weak and has already been discussed when ruling out the external shock origin for the x-ray afterglow. We examine it now within the contexts of a constant density and a wind circumburst medium.

3.1 A constant density medium

For a constant density medium and for $\nu_m < \nu_a < \nu_{\text{obs}} < \nu_c$, $F_{\nu_{\text{obs}}} \propto t^{3(1-p)/4}$ (Sari et al. 1998; Piran 1999). To reproduce the current 8.46 GHz lightcurve $t^{-0.85}$, we need $p \sim 2.1$. The bulk Lorentz factor of the outflow can be estimated by:

$$\Gamma \approx 3.4 E_{k,51}^{1/8} n_0^{-1/8} t_d^{-3/8} (1+z)^{3/8}. \quad (5)$$

The lack of a jet break in the radio afterglow up to 22 days after the burst suggests a very wide jet opening angle $\theta_j > 1$ (Rhoads, 1999; Sari et al, 1999; Halpern et al., 1999).

In the radio band, the synchrotron self-absorption effect should be taken into account. Through the standard treatment (Rybicki & Lightman 1979), for $\nu_a < \nu_m < \nu_c$, we have

$$\nu_a \approx 1.3 \times 10^{10} \text{ Hz } \epsilon_{B,-2}^{1/5} E_{k,51}^{2/5} \epsilon_{e,-1}^{-1} C_p^{-1} (1+z)^{-1} n_0^{3/5}. \quad (6)$$

For $\nu_m < \nu_a < \nu_c$, we have

$$\begin{aligned} \nu_a &\approx 2.6 \times 10^{10} \text{ Hz } \epsilon_{B,-2}^{(p+2)/[2(p+4)]} E_{k,51}^{(p+2)/[2(p+4)]} n_0^{2/(p+4)} \\ &\quad \epsilon_{e,-1}^{2(p-1)/(p+4)} C_p^{2(p-1)/(p+4)} (1+z)^{(p-6)/[2(p+4)]} \\ &\quad t_d^{-(2+3p)/[2(p+4)]}. \end{aligned} \quad (7)$$

With the available radio data, we have three constraints on the physical parameters of the afterglows. One is the self-absorption frequency $\nu_a \sim 4 \times 10^9 \text{ Hz} > \nu_m$ at $t_d \sim 5$. The other is the 22.5 GHz flux $F(22.5 \text{ GHz}) \sim 0.25 \text{ mJy}$ at $t_d \sim 3$. Another is the cooling frequency $\nu_c \leq 5 \times 10^{15} \text{ Hz}$, which has not been presented in Soderberg et al. (2006a) but one can deduce this from their Fig. 2, provided that the synchrotron spectrum of the external shock electrons is not dominated in the XRT band. We thus have the following relations:

$$\begin{aligned} \epsilon_{B,-2}^{(p+2)/[2(p+4)]} E_{k,51}^{(p+2)/[2(p+4)]} n_0^{2/(p+4)} \\ \epsilon_{e,-1}^{2(p-1)/(p+4)} C_p^{2(p-1)/(p+4)} \sim 0.44, \end{aligned} \quad (8)$$

$$\epsilon_{e,-1}^{p-1} \epsilon_{B,-2}^{(p+1)/4} C_p^{p-1} E_{k,51}^{(p+3)/4} n_0^{1/2} \sim 3.2 \times 10^{-3}, \quad (9)$$

$$E_{k,51}^{-1/2} \epsilon_{B,-2}^{-3/2} n_0^{-1} \leq 0.43. \quad (10)$$

These relations are satisfied with $(E_k, \epsilon_e, \epsilon_B, n) \sim (10^{50} \text{ erg}, 0.01, 0.001, 100 \text{ cm}^{-3})$. A similar estimate of ϵ_e has also been suggested by Dai, Zhang & Liang (2006) and is it within the range seen in detailed afterglow modelling of other bursts (Panaitescu 2005).

Fig. 1 depicts our numerical fit to the radio data. The code is the same as that used in Fan & Piran (2006a). One novel effect taken into account is the synchrotron self-absorption, following the standard treatment (Rybicki & Lightman 1979). The external inverse Compton cooling, caused by the long term X-ray emission from the central engine, has been calculated. However, this cooling effect changes the current radio emission only slightly because the inverse Compton parameter $Y_{\text{EIC}} \sim 2L_{\text{ph},41.5} \epsilon_{B,-3}^{-1} E_{k,50}^{-1} t_{d,1}$ (Fan & Piran 2006b) is too small to change the distribution of the shocked electrons significantly (The cooling Lorentz factor is $\sim 10^6$ and the random Lorentz factor electrons accounting for the radio afterglow emission is just \sim a few hundreds). L_{ph} is the luminosity of the X-ray photons from the central source.

Since we are discussing a relatively late radio afterglow at $t_d > 1.8$, and since the kinetic energy is small the fireball is in the sub-relativistic phase at this stage. Therefore the results do not depend on the initial shape of the fireball and

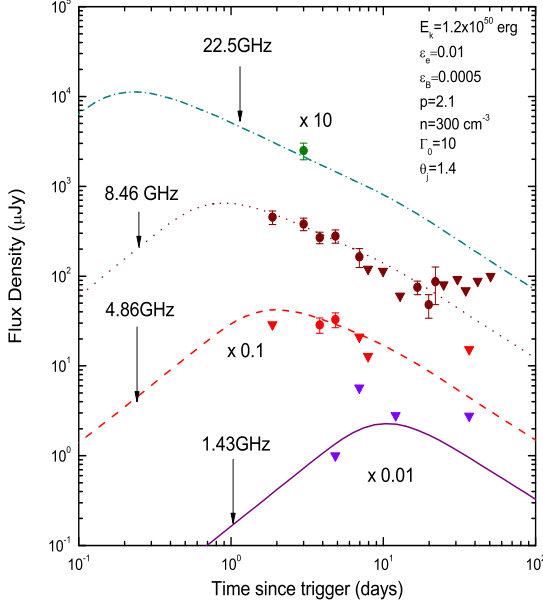


Figure 1. A fit to the observed radio afterglow lightcurves of GRB 060218 (Soderberg et al. 2006a) for a constant density circumburst medium. The inverted triangles are upper limits (3σ). Different colors are for different bands.

in particular the results are insensitive to whether the fireball is thin or thick (Sari & Piran 1995; Lazzati & Begelman 2006).

3.2 A circumburst wind

For a stellar wind (Dai & Lu 1998; Mészáros, Rees & Wijers 1998), $n = 3 \times 10^{35} A_* R^{-2} \text{ cm}^{-3}$, where $A_* = [\dot{M}/10^{-5} M_\odot \text{ yr}^{-1}][v_w/(10^8 \text{ cm s}^{-1})]$ (Chevalier & Li 2000), \dot{M} is the mass loss rate of the progenitor, v_w is the velocity of the wind.

In the relativistic regime the bulk Lorentz factor of the ejecta $\Gamma^w \propto t^{-1/4}$, where the superscript “w” represents the wind model. Following Chevalier & Li (2000), we have the maximal spectrum flux $F_{\nu, \text{max}}^w \propto t^{-1/2}$, $\nu_m^w \approx 1.3 \times 10^{10} \text{ Hz } \epsilon_{e,-1}^2 C_p^2 E_{k,50}^{1/2} \epsilon_{B,-2}^{1/2} (1+z)^{1/2} t_d^{-3/2}$ and $\nu_c^w \approx 3.2 \times 10^{13} \text{ Hz } \epsilon_{B,-2}^{-3/2} E_{k,50}^{1/2} A_*^{-2} (1+z)^{-3/2} t_d^{1/2}$, where $C_p \equiv 13(p-2)/[3(p-1)]$. For $\nu_m^w < \nu_a^w < \nu_{\text{obs}} < \nu_c^w$ (where $\nu_{\text{obs}} = 8.46 \text{ GHz}$ is the observer frequency), as suggested by the observation at $t_d > 1.8$, the observed lightcurve is

$$F_{\nu_{\text{obs}}} = F_{\nu, \text{max}}^w (\nu_{\text{obs}}/\nu_m^w)^{(p-1)/2} \propto t^{(1-3p)/4}. \quad (11)$$

In the Newtonian regime the velocity of the ejecta satisfies $\beta \propto t^{-1/3}$, the radius of the shock front $R \propto t^{2/3}$, the magnetic field strength $B \propto \beta R^{-1} \propto t^{-1}$. Furthermore, we have $F_{\nu, \text{max}}^w \propto RB \propto t^{-1/3}$, $\nu_m^w \propto \beta^4 B \propto t^{-7/3}$, $\nu_c^w \propto t$. Therefore, for $\nu_m^w < \nu_a^w < \nu_{\text{obs}} < \nu_c^w$, we have

$$F_{\nu_{\text{obs}}} \propto t^{(5-7p)/6}. \quad (12)$$

For $p \geq 2$, the resulting temporal indexes are ≤ -1.25 and ≤ -1.5 , (for Eqs. (11) and 12 respectively) are much steeper than the observed slope of -0.85 .

While the $p < 2$ possibility cannot be ruled out but

it is less likely as particles accelerated at relativistic shocks usually have a power law distribution index $p \geq 2$ (Gallant 2002). On the other hand, as shown earlier, in a constant density medium a $p \sim 2.1$ can reproduce the data quite well. So we conclude that a dense wind model is less likely.

4 THE THERMAL EMISSION

A soft thermal component is seen (Campana et al. 2006; Liang et al. 2006) in the X-ray spectrum comprising $\sim 20\%$ of the 0.3-10 keV flux. It begins at $\sim 152 \text{ sec}$ and lasts up to $\sim 10^4 \text{ sec}$. The fitted black body temperature shows a marginal decrease ($kT \simeq 0.16 - 0.17 \text{ keV}$, with k the Boltzmann constant) and a clear increase in luminosity, by a factor of 4 in the time range 300s-2600s, corresponding to an increase in the apparent emission radius from $R_{\text{BB,XRT}} = (5.2 \pm 0.5) \times 10^{11} \text{ cm}$ to $R_{\text{BB,XRT}} = (1.2 \pm 0.1) \times 10^{12} \text{ cm}$ (Campana et al. 2006). In the sharp decline phase, the XRT emission is dominated by a thermal component ($kT = 0.10 \pm 0.05 \text{ keV}$, the corresponding apparent emission radius is $R_{\text{BB,XRT}} = 6.6_{-4.4}^{+14} \times 10^{11} \text{ cm}$). This thermal component is undetectable in later XRT observation.

A second thermal component is detected by the UVOT. At 1.4 days $\sim 120 \text{ ksec}$ the black body peak is centered within the UVOT passband. The fitted values are $kT = 3.7_{-0.9}^{+1.9} \text{ eV}$ and $R_{\text{BB,UVOT}} = 3.29_{-0.93}^{+0.94} \times 10^{14} \text{ cm}$, implying an expansion speed of $(2.7 \pm 0.8) \times 10^9 \text{ cm s}^{-1}$. This speed is typical for a supernova and it is also comparable with the line broadening observed in the optical spectra (Pian et al. 2006). The UVOT thermal component is therefore very likely dominated by the expanded hot stellar envelope (see also Campana et al. 2006).

The nature of the X-ray thermal emission is less clear. Campana et al. (2006) suggest that it arises from a shock break out from a very dense wind ($A_* > 30$) surrounding the SN progenitor. As we have shown earlier the medium surrounding the progenitor is not likely to be a dense wind, as required in this model (Campana et al. 2006). We suggest, therefore, that the XRT thermal component arises from a shock heated stellar matter. As the size of the emitting black body region ($6 \times 10^{11} - 10^{12} \text{ cm}$) is larger than the size of a typical WR- star (10^{11} cm) there are two possibilities: The emission could be from a hot cocoon surrounding the GRB ejecta (Ramirez-ruiz, Celotti & Rees 2002; Zhang et al. 2004) and expanding initially with $v \sim 0.1c$. An alternative possibility is that the X-ray thermal emission arises from the shock break out from the stellar envelope. This would require, however, a progenitor’s size of $\sim 10^{12} \text{ cm}$ (see also Li 2006). This is much larger than $\sim 10^{11} \text{ cm}$ or less, that is expected from a star stripped from its H, He and probably O, as inferred from the spectroscopic analysis of the SNe (Pian et al. 2006). It is not clear if stellar evolution model can accommodate such a progenitor, but surprises of this nature have happened in the past. A relativistic radiation-hydrodynamics calculations are needed to test the viability of these two possibilities. This is beyond the scope of this work.

Here we just show that a hot and optical thick outflow could account for the temporal behavior of the XRT and UVOT thermal emission. After the central engines turns off (i.e., there is no fresh hot material injected), the hot out-

flow expands and cools adiabatically as $T \propto n_p^{1/3} \propto R^{-\alpha/3}$, where $\alpha = 3$ if the hot outflow is spreading and $\alpha = 2$ otherwise, n_p is the number density of the particle. Once the hot region cools adiabatically so that $kT \ll 0.2$ the thermal emission recorded by XRT in the range 0.2 to 10 keV decrease quickly with time as

$$L_{\text{th,XRT}} \propto R^2 e^{-0.2\text{keV}/kT} \propto R^2 e^{-\alpha R/3R_0}, \quad (13)$$

where R_0 is the radius of the outflow at the turning off time of the central engine. The V-band flux is $L_{\text{th,V}} \approx 4\pi\sigma R^2 T^4 \frac{y^3 \Delta y}{e^y - 1}$, where $y = 2.3\text{eV}/kT$, $\Delta y \approx 0.13y$, accounting for the FWHM width of V-band. For $y \ll 1$,

$$L_{\text{th,V}} \propto TR^2 \propto R^{2-\alpha/3} \propto t^{2-\alpha/3}, \quad (14)$$

increases with time until $y \sim 1$ and then it decreases rapidly. As noted by Campana et al. (2006), such a behavior is in agreement with *Swift*'s observations.

5 DISCUSSION AND SUMMARY

The recent nearby burst GRB 060218 had many peculiar features. There are several components of the observed afterglow, X-ray optical and radio and there is no simple afterglow model that can fit two out of the three. From these components only the observed radio afterglow at $t \sim 10^5$ sec is rather usual and its lightcurve is compatible with a weak burst with a low kinetic energy. We summarize the situation below:

- The temporal decay of the bright (non-thermal) X-ray afterglow ($t > 10^4$ s) looks like typical. However, the very steep spectrum and the very weak radio afterglow rule out an external shock origin (both from synchrotron radiation and from inverse Compton emission). We suggest following the earlier suggestion of Katz & Piran (1997) and Katz, Piran & Sari (1998) that this emission arises due to continued activity of the central engine. This is the first time that a power-law decaying X-ray afterglow is attributed to the activity of the central engine, though it has been suggested (Fan & Wei 2005; Zhang et al. 2006) that the flare-rich X-ray afterglow that have been detected in a good fraction of *Swift* GRBs (O'Brien et al. 2006) also trace the long term activity of the central engine.
- The radio afterglow can be understood within the standard fireball blast wave model, provided that the medium is ISM-like, the overall kinetic energy is 10^{50} erg, and the fraction of shock energy given to the electrons is ~ 0.01 . A wind profile is disfavored as it requires $p \sim 1.5$ and even then it is not clear if one can reproduce the observation.
- The lack of a “jet break” of 8.46 GHz afterglow lightcurve up to 22 day indicates that the outflow is very wide ($\theta_j > 1$). This is somewhat at odds with the standard Collapsar model that involves a narrow jet.
- The X-ray and optical/UV thermal emission cannot arise from the relativistic ejecta. A shock heated envelope of the progenitor is the most natural source. The question whether the envelope has expanded rapidly or was it initially large is open.

There are several implications to these conclusions. First we note that in the current event, the long term power-law decaying X-ray afterglow, the ultraviolet/optical after-

glow and the radio afterglow cannot be attributed to the same physical process and they arise from different regions. While this is sort of expected for the thermal optical and X-ray components it is somewhat puzzling and alarming that the two nonthermal X-ray and radio components do not seem to arise from the same source. While it may indicate a serious problem in the overall fireball model we suggest that this is a manifestation of the fact that GRBs are much more complex than was anticipated earlier and that indeed different components such as external shocks as well as continued activity of the central engine might take place simultaneously. Of course GRB 060218 is not unique in this case and such a complexity might have been seen in other peculiar multi-wavelength afterglows which have been poorly interpreted within the standard external shock model (Fan & Piran 2006a).

We have argued that there is a clear indication that a power-law decaying, non-thermal X-ray afterglow that cannot be produced by an external shock and we have shown in §2 that fall-back accretion within a collapsar might be energetic enough to power a detectable “central engine afterglow”. This component is in particular important for the sub-luminous GRBs, for which the ejecta is significantly less energetic than that of the typical GRBs and the late activity of the central engine is not hidden by the external shock afterglow. Such sub-luminous GRBs can be detected only from small distances. As it is possible and even likely (Nakar 2006, private communication) that the real rate of such GRBs is significantly higher than the rate of regular GRBs they should dominate the nearby bursts population. We thus predict that such central engine afterglow would be detected in a good fraction of nearby GRBs. In fact with a slight change of the parameters it is possible that the central engine afterglow might dominate over the external shock afterglow even for brighter GRBs. This, for example, could arise in GRB 060210.

The power-law decaying “central engine afterglow” of GRB 060218 was identified by its very steep X-ray spectrum. However, the inconsistency of the strong X-ray afterglow with the weak radio signal was essential to verify this idea. In general the X-ray spectrum of the central engine afterglow is not necessarily so steep. For example, within the well detected X-ray flares, that have been attributed to continued activity of the central engine, just a few have a very steep spectrum (see Table 8 of Bulter 2006). Therefore, a multi-wavelength afterglow analysis is essential to identify the “central engine afterglow” component.

Finally we mention two observed features that seem to be inconsistent with the canonical Collapsar model. The first among the two is the lack of a clear wind profile. The afterglows arises at a distance of $R \sim 10^{17}$ cm from the central engine. It could be that the observed profile arose from the interaction of the wind with the surrounding matter or it may reflect a low mass-loss rate of the progenitor star during the post-helium burning phases. A similar feature was seen also in many GRBs but here we have information on regions that are nearer to the central engine. The wide angle of the relativistic ejecta is also incompatible with the usual Collapsar model, in which a narrow jet punches a narrow hole in the envelope of a WR star (Zhang et al. 2004). This may indicate that GRB 060218 was an almost “failed GRB”. Due to some unique feature of the progenitor (a larger than

usual size? or a smaller than typical mass?) the relativistic ejecta almost did not make it across the envelope. This has lead to a wide relativistic outflow with an unusually low initial Lorentz factor. This, in turn, lead to the softer spectrum (possibly due to internal shocks taking place in a region with optical depth of order unity). A significant fraction of the energy was given to a hot cocoon and was reprocessed as a thermal emission - seen both in X-ray and later in the UV/optical. One can speculate that in many other cases the relativistic ejecta would have stopped completely and we would have a “failed GRB”. It is possible that this is the reason why GRBs are not seen in most type Ib, c SNe (Berger et al., 2003, Soderberg et al., 2006b).

ACKNOWLEDGMENTS

We thank E. Waxman for helpful discussions and an anonymous referee for comments. This work is supported by US-Israel BSF and by the ISF via the Israel center for High Energy Astrophysics. TP acknowledges the support of Schwartzmann University Chair. YZF is also supported by the National Natural Science Foundation (grants 10225314 and 10233010) of China, and the National 973 Project on Fundamental Researches of China (NKBRF G19990754). DX is at the Dark Cosmology Center funded by The Danish National Research Foundation.

REFERENCES

- Berger E., et al. 2003, *ApJ*, 599, 408
 Bulter N. R., 2006, *ApJ*, submitted (astro-ph/0604083)
 Chevalier R. A., Li Z. Y., 2000, *ApJ*, 536, 195
 Campana S., et al., 2006, *Nature*, in press (astro-ph/0603279)
 Colgate S. A., 1974, *ApJ*, 187, 333
 Cusumano G., et al., 2006a, *GCN Circ.* 4775
 Cusumano G., et al., 2006b, *GCN Circ.* 4786
 Dai Z. G., Lu T., 1998, *MNRAS*, 298, 87
 Dai Z. G., Zhang B., Liang E. W., 2006, *ApJL*, submitted (astro-ph/0604510)
 De Luca A., 2006, *GCN Circ.* 4853
 Fan Y. Z., Piran T., 2006a, *MNRAS*, 369, 197
 Fan Y. Z., Piran T., 2006b, *MNRAS Letters*, in press (astro-ph/0601619)
 Fan Y. Z., Wei D. M., 2005, *MNRAS*, 364, L42
 Gallant, Y. A., 2002, *Lecture Notes in Physics*, 589, 24
 Halpern J. P., Kemp J., Piran T., Bershadsky M. A., 1999, *ApJ*, 517, L105
 Katz J. I., Piran T., 1997, *ApJ*, 490, 772
 Katz J. I., Piran T., Sari R., 1998, *Phys. Rev. Lett.*, 80, 1580
 Lazzati D., Begelman M. C., 2006, *ApJ*, 641, 972
 Li L. X., 2006, *MNRAS*, submitted (astro-ph/0605387)
 Li Z. Y., Chevalier R. A., 1999, *ApJ*, 526, 716
 Liang E. W., Zhang B., Zhang B. B., Dai Z. G., 2006, *Nature*, submitted (astro-ph/0606565)
 MacFadyen A. I., Woosley S. E., Heger A., 2001, *ApJ*, 550, 410
 Mazzali, P. A., Deng, J. S., Nomoto K., Pian, E., Tominaga, N., Tanaka, M., Maeda, K., 2006, *Nature*, submitted (astro-ph/0603567)
 Mészáros P., Rees M. J., Wijers R. A. M. J., 1998, *ApJ*, 499, 301
 Mirabal N. et al., 2006, *ApJ*, 643, L99
 Mirabal N., Halpern J. P., 2006, *GCN Circ.* 4792
 Modjaz M., et al., 2006, *ApJL*, submitted (astro-ph/0603377)
 O’Brien P. T., et al., 2006, *ApJ*, submitted (astro-ph/0601125)
 Panaitescu A., 2005, *MNRAS*, 363, 1409
 Pian E., et al., 2006, *Nature*, submitted (astro-ph/0603530)
 Piran T., 1999, *Phys. Rep.*, 314, 575
 Ramirez-ruiz E., Celotti A., & Rees M. J., 2002, *MNRAS*, 337, 1349
 Rhoads, J. E. 1999, *ApJ*, 525, 737
 Rybicki, G. B., & Lightman, A. P., 1979, *Radiative Processes in Astrophysics* (New York: Wiley)
 Sakamoto T., et al., 2006, *GCN Circ.* 4822
 Sari R., Narayan R., Piran T., 1996, *ApJ*, 473, 204
 Sari R., Piran T., 1995, *ApJ*, 455, L143
 Sari R., Piran T., Narayan R. 1998, *ApJ*, 497, L17
 Sari R., Piran T., Halpern J. P., 1999, *ApJ*, 519, L17
 Soderberg A., et al. 2006a, *Nature*, submitted (astro-ph/0604389)
 Soderberg A., et al. 2006b, *ApJ*, 638, 930
 Sollerman J., et al., 2006, *A&A*, in press (astro-ph/0603495)
 Stanek, K. Z. et al., 2006, *ApJL* submitted (astro-ph/0602495)
 Waxman E., 2004, *ApJ*, 605, L97
 Wei D. M., Lu T., 1998, *ApJ*, 505, 252
 Woosley S. E., Zhang W. Q., Heger A., 2003, *AIPC*, 662, 185
 Yost S., Harrison F. A., Sari R., Frail D. A., 2003, *ApJ*, 597, 459
 Zhang B., Fan Y. Z., Dyks J., Kobayashi S., Mészáros P., Burrows D. N., Nousek J. A., Gehrels N. 2006, *ApJ*, 642, 354
 Zhang W. Q., Woosley S. E., Heger A., 2004, *ApJ*, 608, 305